

Interleaved Fly Back Micro-Inverter with Primary Side Current Control For PV System

Mamidi Bharathi

Assistant Professor

D.M.S.S.V.H. College of Engineering, Machilipatnam

Abstract - In this paper, the interleaved fly back inverter is proposed following the topology has been broadly utilized for PV system tied small scale inverter applications. The small scale inverter arrangement permits controlling each photovoltaic (PV) module freely and diminishing the crisscross misfortune, which is regular in string and utility inverters. Fly back inverter generally works in intermittent conduction mode (NCM) or limit conduction mode (LCM) because of its straightforwardness in controller outline. In this study, the controller has been intended for continuous conduction mode (CCM) operation keeping in mind the end goal to diminish part push and build power thickness. The present control depends on the essential side, which is an aberrant regulation for the network outpouring. A little flag model is likewise created for the controller combination. Reproduction confirms the execution of the proposed inverter.

Keyword - Continuous conduction mode, Intermittent conduction mode, PV module.

I. INTRODUCTION

PV smaller scale inverter is getting to be main stream because of unsolvable brought together most extreme power point following (MPPT) confounding issue amid incomplete shading circumstances [1-4]. This confounds impact causes a lot of power misfortune as the PV modules in arrangement association are not working at their particular greatest influence point (MPP). Module incorporated converter system is hence proposed to conquer the issue [5]. With every board is streamlined with its own particular MPP Tracker (MPPT), the determination is higher. In this manner the system accomplishes higher effectiveness. Such systems are called as AC Modules (ACM), module coordinated converter (MIC) or smaller scale inverters. A few smaller scale inverter topologies are presented for PV applications. Transformer-less ones came up for its little size, yet they have issue with the board's parasitic capacitor [6]. Likewise a DC-join capacitor is required in the middle of the inverter and the converter. Powerlessness to scale its yield voltage into a few times higher additionally makes the topologies unrealistic to serve in nations with high system voltage. To defeat the voltage boosting issue, falling disconnected converter to an inverter is proposed [7]. It doesn't just comprehend the voltage issue; it additionally has high effectiveness and long lifetime.

However, the topology accompanies an expense of more parts and muddles its control issue. There is another choice. A confined converter beside the board shapes its yield into semi-sinusoid waveform. It then joins with a low recurrence unraveling inverter to flip the extremity making the yield sinusoidal waveform. Thusly the DC-join capacitor is decreased to just the one by the board. Furthermore, beside the MPPT, the main control undertaking is on the DC-DC converter to shape its yield as coveted. Fly-back converter has its element like that of buck-support converter; however it uses a transformer to give an expansive voltage venture up proportion and galvanic disconnection. Because of the presence of a non-least stage (NMP) zero [8] and system element issue [9] in CCM, the topology has rather been intended to work in DCM. In return for basic element, there exist a few downsides to confuse the topology with a specific end goal to make DCM functional. Furthermore, DCM additionally just works amid light load condition, making misuse of the gadgets ability to change over more power. Because of DCM issues, fly-back inverter in BCM is proposed. It confounds the control calculation; however it can change over more power and straightforwardness gadget anxiety issue. In any case, BCM is just conceivable in high power range; generally the inverter will work in DCM. Hence blend of operation is recommended for such systems [10, 11]. The control issue for CCM, then again, has as of late been overcome by utilizing a straightforward simple controller [8, 12] for the present controller. Another technique is testing the yield from lattice side channel rather [9], making it conceivable to control the system utilizing computerized controller. In both cases, a sort 2 compensator is used in the present control circle. The control issue is along these lines demonstrated to not be an issue and the controller is streamlined. Despite the fact that the system is composed under CCM operation, it likewise works exceptionally well in DCM amid network voltage extremity moving period [12]. These plans intentionally enhance the topology productivity; however bends in the yield current are likewise there [8, 9, 12].

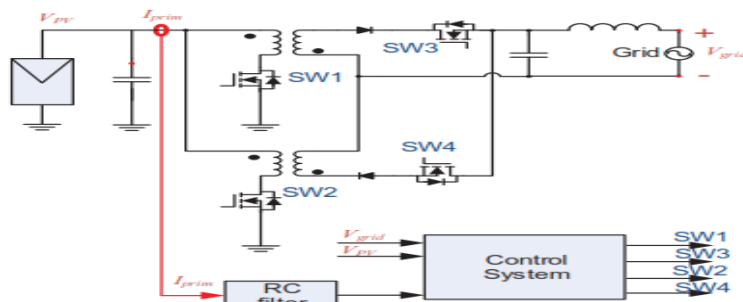


Figure 1: Proposed system

This paper offers a topology for interleaved fly-back miniaturized scale inverter sharing two regular switches and matrix side channel with different converters from diverse boards. To do as such, essential current control plan is required [8].

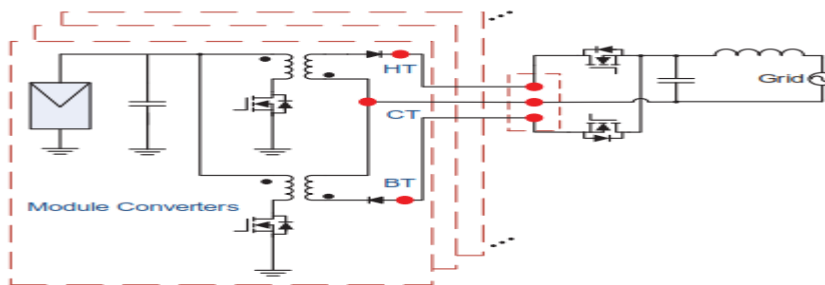


Figure 2: Multiple fly back micro-inverter interconnected

On the other hand, the present streaming at the essential side is an exchanging sign after the exchanging recurrence. This represents a trouble issue to execute computerized control. In this way this paper additionally proposes setting a channel on the input way to smoothen the sign while as yet keeping up great control result.

II. PROPOSED INTERLEAVED FLY BACK MICRO-INVERTER

The proposed topology's schematic is appeared in Figure 1. The power is drawn from the PV board and its capacitor through the power train in changing way to bolster the system. The capacitor arrives to bolster board voltage and channel its energy when the topology is quickly dormant to expand the yield. Keeping in mind the end goal to accomplish the individual MPP, the essential current is controlled to shape its optional side current into sinusoid waveform. In this way the system can be built as appeared in Figure 2. In this topology, two transformers are utilized and work independently. SW1 is utilized alongside its transformer amid the positive half cycle with SW3 initiated. The other two switches are impaired amid this half period. Furthermore, when the control system recognizes negative voltage from the matrix, SW1 and SW3 are incapacitated. In the negative half, SW2 is utilized for the forming and SW4 remains empowered.

To accomplish free MPPT and decrease the part tallies, the brace side segments are intended to be shared by a gathering of parallel joined inverter units. Figure 2 shows the basic focuses where alternate modules can bury associated from their individual HT, CT, and BT joints to the lattice side switches and channel. The microcontroller is shared amongst the module converters to the extent its ability goes.

2.1 Control Structure

The general control system chart is appeared in Figure 3.

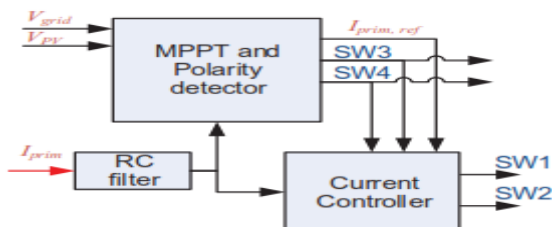


Figure 3: Proposed overall control system

The MPPT is in charge of conforming the top reference signal for the current control system. The reference sign is then differing itself as per the network stage. The extremity indicator deals with SW3 and SW4 actuation.

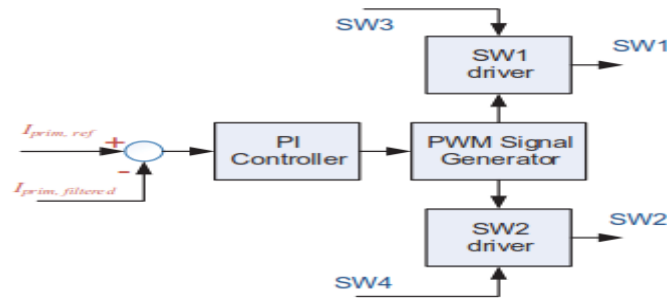


Figure 4: Current controller

Hence one microcontroller can deal with various converters to the extent its ability goes. With a specific end goal to minimize module utilization of the microcontroller, stand out heartbeat width adjustment (PWM) module is used per converter. As needs be, the current control system takes the reference signal, as well as SW3 and SW4 empowering signal too.

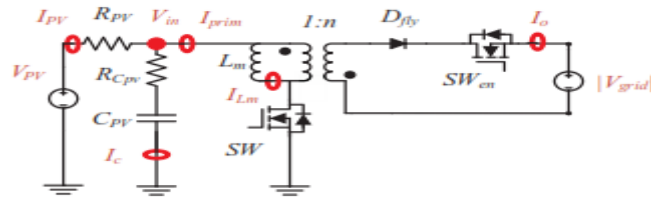


Figure 5: Dynamic model equivalent circuit

The momentum controller part contains a PI controller, PWM signal generator, and SW1 and SW2 driver. The initial two parts are evidently inserted in the microcontroller. This present controller chart is appeared in Figure 4. The controller takes the reference signal from MPPT calculation and contrasts it and the separated exchanging signal. The control sign is bolstered to PWM module where it creates PWM sign to switch driver IC. The driver for SW1 takes SW3 enactment signal into its empowering pin and SW4 is as needs be for SW2.

III. ELEMENT MODELING AND CONTROL DESIGN

3.1 Photovoltaic Model

Normal for a photovoltaic is nonlinear, particularly at its MPP. An expression for the PV current is appeared as in mathematical statement (1) [13].

$$i_{pv}(t) = I_{pv} - I_o \left(e^{\frac{V_{pv} + R_s i_{pv}}{V_t a}} - 1 \right) - \frac{V_{pv} + R_s i_{pv}}{R_p} \tag{1}$$

where i_{pv} and I_o are the output current and saturation current of a module, $V_t = \frac{kT}{q}$ is the thermal voltage with s N cells connected in series, k is the Boltzmann constant, q is the electron charge, T is the cell temperature, s R is the equivalent shunt resistance, and a is the ideality constant of the diode.

Considering that the system for the most part works at MPP, the PV module has been linearised around its MPP as appeared in Figure 5 [8, 9]. The PV board is spoken to as the DC voltage source and a resistor. The network is supplanted with a fluctuating DC voltage source subsequent to, if the system works appropriately, the topology is just presented to positive optional side voltage. The red rings imply current sensors with its bearing from dark line on top to red line on top.

3.2 Fly back Inverter Modeling

Small signal averaged model approach is used for modeling the inverter. Equation (2)-(5) shows the basic relationship between each parameter in the system. Each of the parameters is delineated in Figure 5. The bar symbol signifies average variable.

$$\overline{V_{Lm}} = \overline{d} \cdot \overline{V_{in}} - \frac{1-\overline{d}}{n} \cdot |V_{grid}| \tag{2}$$

$$\overline{i_{pv}} = \overline{i_c} + \overline{i_{prim}} \tag{3}$$

$$\overline{i_{prim}} = \overline{d} \cdot \overline{i_{Lm}} \tag{4}$$

$$\overline{V_{in}} = \overline{V_{Cpv}} + \overline{V_{Rcpv}}$$

where Lm v is the magnetizing inductor voltage, d is the duty ratio enacted on SW , in v is the panel's terminal voltage, n is the transformer turns ratio, $grid$ V is momentarily grid voltage, pv i is the panel current, c i is the capacitor current, $prim$ i is the switching current, Cpv v is the capacitor voltage, and $Rcpv$ v is the capacitor's ESR voltage.

The average variables in the mathematical statements above is isolated into two sections for small signal modeling demonstrating as appeared in comparison (6). The mathematical statements above are then utilized for growing second-order state space equation comparison as in mathematical statement (7). The cap image connotes little changes in the variable and the capital means its linearised point. The model is then constructed by parameters in Table 1 for control outline reason.

$$\overline{\bar{x}} = X + \hat{x} \tag{5}$$

$$\begin{bmatrix} \widehat{v_{Lm}} \\ \widehat{v_{Cpv}} \end{bmatrix} = A \begin{bmatrix} \widehat{v_{Lm}} \\ \widehat{v_{Cpv}} \end{bmatrix} + B \widehat{d} \tag{6}$$

$$\widehat{v_{sw}} = C \begin{bmatrix} \widehat{v_{Lm}} \\ \widehat{v_{Cpv}} \end{bmatrix} + D_o \widehat{d} \tag{7}$$

$$A = \begin{bmatrix} \frac{-D^2 R_{pv} R_{Cpv}}{L_m(R_{pv} + R_{Cpv})} & \frac{-D R_{pv}}{L_m(R_{pv} + R_{Cpv})} \\ \frac{-D R_{pv}}{C_{pv}(R_{pv} + R_{Cpv})} & -1 \end{bmatrix}; \tag{8}$$

$$B = \begin{bmatrix} \frac{V_{Cpv} R_{pv} - 2 D I_{Lm} R_{pv} R_{Cpv} + V_{pv} R_{Cpv}}{L_m(R_{pv} + R_{Cpv})} + \frac{|V_g|}{L_m n} \\ \frac{-I_{Lm} R_{pv}}{C_{pv}(R_{pv} + R_{Cpv})} \end{bmatrix}; \tag{9}$$

$$C = [D \ 0]; \tag{10}$$

$$D = -I_{Lm}; \tag{11}$$

3.3 Signal Filter

A simple resistive-capacitive filter is inserted in the feedback path to smoothen the signal. Figure 6 illustrates the proposed filter. Rs represent infinity resistance of control devices. The filter transfer function is derived as shown in equation (9) where $R \ll 1$ kΩ and $C \ll 0.06$ μF. Although this additional filter introduces delay in the control loop, this pole later is compensated by a zero in the controller.

$$H_{filter}(s) = \frac{1}{R.C.s + 1}$$

Table 1: The case study parameters

Name	Symbol	Value
Transformer Inductance	L_m	28μH
Transformer Turns Ratio	N	12
Output Inductor	L_f	4mH
Output Inductor's DCR	R_{Lf}	1.18ohms
Output Capacitor	C_f	0.22 μF
Output Capacitor's ESR	R_{cf}	0.02ohms
PV Capacitor	C_{pv}	4.7mF
PV Capacitor's ESR	R_{Cpv}	0.02ohms
Primary Filter Capacitor	C_p	0.06 μF
Primary Filter resistor	R_p	1Kohms
Grid RMS voltage	$V_{g,rms}$	220V
Grid frequency	f_g	60HZ
Switching frequency	f_{sw}	170KHZ
Duty ratio	D	0.3

This similar transfer function exists in both [8] and [12] as part of PI type 2 controllers, but placing in the feedback path makes it possible to control the system using digital controller.

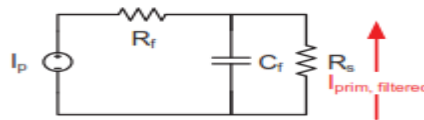


Figure 6: RC filter

The signal sensed from this filter can also be used for MPPT purpose. This transfer function is then added to the switching current's model as derived in the equation (7) and (8) directly.

3.4 Control Design

Assuming the power train has very low loss, the power drained from the panel should be the same as transmitted to the grid. The reference signal for the controller is thus not a step signal, but a squared sinusoid [8]. However, considering that the switching frequency is much higher than the grid frequency, the reference signal can be treated as a step signal in a short time. The whole term for amplitude could be manipulated according to MPPT result. With equation (12) as the reference, the controller is required to act multiple times faster than the grid frequency. Controller design is carried out using MATLAB's 'PIDTOOL' in order to acquire the optimal parameters with the requirement. The controller's bandwidth is chosen at 20 kHz with 75 degree phase margin. Figure 7 shows the closed loop response for the acquired controller with the model. The resulting controller, using data shown in Table 1, is presented in equation (13). This controller is placed and works as 'PI Controller' block in Figure 3.

$$P_g(t) = 2 \cdot V_{rms} I_{rms} \sin^2 \omega t \tag{12}$$

$$P_{pv}(t) = v_{pv}(t) \cdot i_{sw}(t) \tag{13}$$

$$i_{sw}(t) = \frac{2 \cdot V_{rms} I_{rms}}{V_{pv}} \cdot \sin^2 \omega t \tag{14}$$

$$C(s) = 1.33 \left(\frac{1+4.9e^{-5.s}}{4.9e^{-5.s}} \right) \tag{15}$$

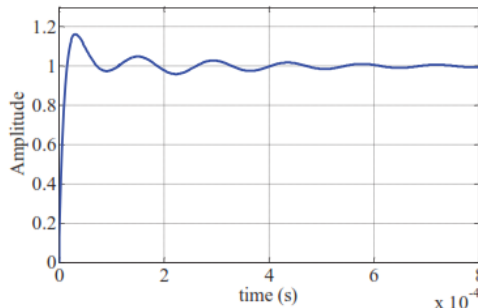


Figure 7: Closed loop step response

IV. SIMULATION & RESULTS

The system is simulated using PSIM software with snubber circuit and parasitic components. The controller designed in the previous section is implemented as in equation (13) and described in section 2.

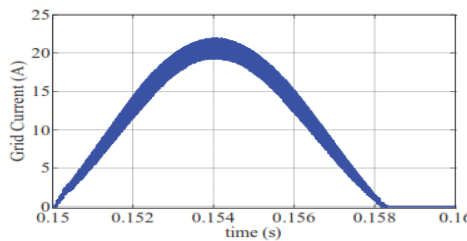


Figure 8: Magnetizing current

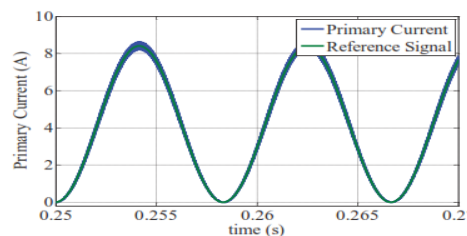


Figure 9: Primary current control result

The simulation results are shown in Figure 8 to Figure 11. However, it is in DCM during the time it rises from zero as it just starts charging the magnetizing inductor. Figure 9 illustrates the simulation result for the primary current. The control objective is achieved as the averaged switching current follows its rotating reference signal closely. Figure 10 shows the grid voltage and the current feeding into the grid. Although the grid current follows grid voltage closely, there are noticeable distortions around polarity shifting points. This however does not affect its THD significantly.

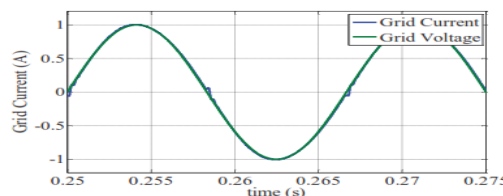
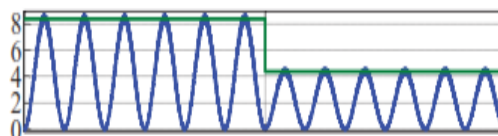


Figure 10: Grid current control result Primary Current (A)

Grid current's THD satisfyingly results in only 2 percent compared to the grid code of 5 percent [14].



Output Current (A)

Additionally, the feedback filter does not heavily affect the performance as well since its PF is at 99.9 percent in Figure 10. This shows improvement from previous literature work [8, 12].

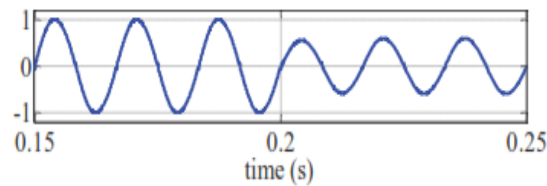


Figure 11: Primary Current Reference Shifting

Figure 11 shows the simulation results with the system experiences a peak value shift at 0.2s from 8.4 A to 4.4 A. Both the primary current and output current adjust into their respective transient operation quickly using just a grid cycle time.

V. CONCLUSION

In this work, a fly back inverter with sharing developing switches has been proposed alongside its control plan. The fundamental motivation behind this work is to control the essential current sign keeping in mind the end goal to utilize miniaturized scale controller for network tied operations. A low recurrence RC channel is included as a component of the criticism way. A second request little flag model is then created for control outline reason alongside the channel model. MATLAB is utilized a while later for control outline. The framework is then exhibited by reenactment in PSIM programming with commonsense model. The reproduction results in great execution fulfilling the lattice codes with 2% THD, and 99.9% PF. The control system likewise adjusts quickly with change in reference top quality as impact from MPPT calculation.

VI. REFERENCES

- [1] Y. Du and D. D.-C. Lu, "Battery-integrated boost converter utilizing distributed MPPT configuration for photovoltaic systems," *Solar Energy*, vol. 85, pp. 1992-2002, 2011.
- [2] H. Häberlin, "Solar Modules and Solar Generators," in *Photovoltaics System Design and Practice*, ed: John Wiley & Sons, Ltd, 2012, pp. 127-221.
- [3] A. Mäki and S. Valkealahti, "Power Losses in Long String and Parallel-Connected Short Strings of Series-Connected Silicon-Based Photovoltaic Modules Due to Partial Shading Conditions," *IEEE Trans. on Energy Conv.*, vol. 27, pp. 173-183, 2012.
- [4] H. Patel and V. Agarwal, "MATLAB-Based Modeling to Study the Effects of Partial Shading on PV Array Characteristics," *IEEE Trans. on Energy Conv.*, vol. 23, pp. 302-310, 2008.
- [5] J. J. Bzura, "The AC module: An overview and update on self-contained modular PV systems," in *Power and Energy Society General Meeting*, 2010, pp. 1-3.
- [6] R. Teodorescu, M. Liserre, and P. Rodríguez, "Photovoltaic Inverter Structures," in *Grid Converters for Photovoltaic and Wind Power Systems*, ed: John Wiley & Sons, Ltd, 2011, pp. 5-29.
- [7] C. Rodriguez and G. Amaratunga, "Long-Lifetime Power Inverter for Photovoltaic AC Modules," *IEEE Trans. on Ind. Elec.*, vol. 55, pp. 2593-2601, 2008.
- [8] T. V. Thang, N. M. Thao, J. Jong-Ho, and P. Joung- Hu, "Analysis and Design of Grid-Connected Photovoltaic Systems With Multiple-Integrated Converters and a Pseudo-DC-Link Inverter," *IEEE Trans. on Ind. Elec.*, vol. 61, pp. 3377-3386, 2014.
- [9] F. F. Edwin, W. Xiao, and V. Khadkikar, "Dynamic Modeling and Control of Interleaved Flyback Module-Integrated Converter for PV Power Applications," *IEEE Trans. on Ind. Elec.*, vol. 61, pp. 1377-1388, 2014.
- [10] X.-F. He, Z. Zhang, and X. Li, "An optimal control method for photovoltaic grid-connected interleaved fly back micro-inverters to achieve high efficiency in wide load range," in *7th In'l Power Elec. and Motion Control Conf. (IPEMC)*, 2012, pp. 1429-1433.
- [11] Z. Zhang, X.-F. He, and Y.-F. Liu, "An Optimal Control Method for Photovoltaic Grid-Tied- Interleaved Fly back Micro inverters to Achieve High Efficiency in Wide Load Range," *IEEE Trans. on Power Elec.*, vol. 28, pp. 5074-5087, 2013.
- [12] Y. Li and R. Oruganti, "A Low Cost Flyback CCM Inverter for AC Module Application," *IEEE Trans. on Power Elec.*, vol. 27, pp. 1295-1303, 2012.
- [13] M. G. Villalva, J. R. Gazoli, and E. R. Filho, "Comprehensive Approach to Modeling and Simulation of Photovoltaic Arrays," *IEEE Trans. on Power Elec.*, vol. 24, pp. 1198-1208, 2009.
- [14] G. Petrone, G. Spagnuolo, R. Teodorescu, M. Veerachary, and M. Vitelli, "Reliability issues in Photovoltaic Power Processing Systems," *IEEE Trans. on Ind. Elec.*, vol. 55, pp. 2569-2580, 2008.